Melting and superheating of sI methane hydrate: Molecular dynamics study

Grigory S. Smirnov and Vladimir V. Stegailov

Citation: J. Chem. Phys. **136**, 044523 (2012); doi: 10.1063/1.3679860
View online: http://dx.doi.org/10.1063/1.3679860
View Table of Contents: http://jcp.aip.org/resource/1/JCPSA6/v136/i4
Published by the American Institute of Physics.

Melting and superheating of sI methane hydrate: Molecular dynamics study

Grigory S. Smirnov[1,a)] and Vladimir V. Stegailov[2,b)]
[1]*Joint Institute for High Temperatures of RAS, 125412 Moscow, Russia*
[2]*Moscow Institute of Physics and Technology, 141700 Dolgoprudny, Russia*

(Received 19 August 2011; accepted 9 January 2012; published online 31 January 2012)

Melting and decay of the superheated sI methane structure are studied using molecular dynamics simulation. The melting curve is calculated by the direct coexistence simulations in a wide range of pressures up to 5000 bar for the SPC/E, TIP4P/2005 and TIP4P/Ice water models and the united-atom model for methane. We locate the kinetic stability boundary of the superheated metastable sI structure that is found to be surprisingly high comparing with the predictions based on the classical nucleation theory. © *2012 American Institute of Physics*. [doi:10.1063/1.3679860]

I. INTRODUCTION

Gas hydrates are crystalline water-based inclusion compounds physically resembling ice.[1] Gas hydrates have been found in gas pipelines,[2] permafrost regions, ocean sediments, comets, and certain outer planets.[3,4] Guest molecules such as CH_4, Ar, and CO_2 are trapped inside cavities of the hydrogen-bonded water network. Natural gas hydrates are classified into three structures: a cubic structure sI,[5] a face-centered cubic structure sII,[6] and a hexagonal structure sH.[7] The structure type is mainly determined by the size of guest molecules. Methane hydrate at normal conditions has a sI structure with a unit cell composed of six $5^{12}6^2$ and two 5^{12} polyhedra with an O atom at each vertex and H atoms located at the edges.

Gas hydrates allow compact storage of hydrocarbons since one volume of hydrate may contain 180 volumes of gas (STP). The abundance of methane hydrate in nature makes it a promising future energy resource, but at the same time it leads to a "clathrate gun hypothesis"[8] that the rise of the sea temperature could trigger a sudden methane release from hydrates that subsequently could lead to further temperature rise and massive destabilization of the methane hydrate sediments. Gas hydrates are also considered as a possible solution for sequestrating of CO_2 from the atmosphere.[9–13] Recently, sII and sH gas hydrates have attracted interest due to the possibility of being used for hydrogen storage.[14–20]

The importance of methane hydrate requires the accurate knowledge of their thermodynamic and kinetic properties, mechanisms of formation and decay. Molecular simulation is a method of choice for such theoretical studies since it can explicitly capture the structure of gas hydrates and their constituents. Molecular dynamic (MD) simulation was used to study different processes in methane hydrate.[21–34] Tung *et al.*[34] determined the coexistence line in a wide range of pressures using TIP4P/Ew water model[35] and OPLS-AA model[36] for methane. They analyzed the evolution of the potential energy as a function of time during NPT simulations. The increase in potential energy indicated melting, whereas its decrease indicated crystallization. The resulting equilibrium phase coexistence temperature was taken as an average of the lowest temperature at which the hydrate melted and the highest temperature at which the system freezed. Repeating such simulations at different pressures gave the melting temperature as a function of pressure. Conde and Vega[37] used a similar technique to determine the coexistence points at up to 400 bar. They established that the TIP4P/Ice model[38] gives the best agreement with the experimental results but their results differ from the Monte Carlo data of Jensen *et al.*[39]

In this work, we perform coexistence simulations for pressures up to 5000 bar for different water models. We calculate the kinetic stability boundary of the superheated metastable sI structure and analyze the effects of the heating rate, system size and cage occupancy.

II. MODEL

To obtain the initial coordinates of oxygen atoms, we use the crystallographic data[40] (the unit cell contains 46 water and 8 methane molecules). Methane molecules are centered in the cages of sI. The cages are fully occupied. We consider the case of the partial cage occupancy separately. Initial coordinates of hydrogen atoms are chosen in a way that creates a continuous network of hydrogen bonds with a zero net dipole moment and a zero net quadrupole moment.[41]

The state-of-art classical potentials allow quite accurate overall description of the water phase diagram in the solid phase.[42] Important features of water can be captured even by simplified potential models.[43–45] The recent work of Jiang *et al.*[46] shows that the polarizable force field represents more accurately the radial distribution function and the temperature dependence of the lattice constant of methane hydrate. However, since our priority is the description of the phase diagram we use the TIP4P/Ice[38] model that gives a very good description of the ice phases coexistence lines. For comparison, we consider TIP4P/2005[47] and a well-known SPC/E[48] model. SPC/E is a simple 3-site model with charges located on H and O sites. TIP4P models are the 4 site models with a negative massless charge located near the oxygen atom and positive charges located on H atoms. We use a simple Lennard-Jones (LJ) model for methane proposed by Guillot and Guissani[49]

a)Electronic mail: grsmirnov@gmail.com.
b)Electronic addresses: stegailov@ihed.ras.ru and stegailov@gmail.com.

and Paschek.[50] Sun and Duan[51] developed an *ab initio* based all-atom potential for methane in hydrate but it requires essentially larger computational effort with somewhat uncertain gain in accuracy for phase diagram studies.

The cross interaction between methane and water is described by the Lorentz-Berthelot rules $\varepsilon_{CH_4-H_2O} = \chi\sqrt{\varepsilon_{CH_4-CH_4}\varepsilon_{H_2O-H_2O}}$, $\sigma_{CH_4-H_2O} = (\sigma_{CH_4-CH_4} + \sigma_{H_2O-H_2O})/2$, where $\chi = 1$ or 1.07. The latter value describes the chemical potential of methane in TIP4P/2005 water better.[52] We test different cutoff distances from 9 to 13 Å for the LJ and Coulombic potentials. No difference was found. The particle-particle-particle-mesh algorithm[53] is applied to take into account the long-range interactions. Water molecule bonds and angles are fixed using the SHAKE algorithm. The 3D periodic boundary conditions are used. The integration time step is 2 fs. All MD calculations are performed using LAMMPS.[54]

III. EQUILIBRIUM MELTING

First, we determine coexistence equilibrium temperatures and pressures. Conde and Vega in their recent work[37] performed similar calculations using long NPT MD trajectories (up to 1 μs). At several fixed temperatures, they waited for complete crystallization or complete melting of the initial three-phase system. We follow another approach looking directly for the phase coexistence conditions.[57,58] At the preliminary stage in our calculations, one half of the system is melted while another half is frozen. Then a short NPT simulation is performed to drive the system to the desired temperature and pressure. Finally, the system evolve for several nanoseconds in the NVE MD run. Depending on the initial kinetic energy of the system one can observe either melting or growth of the sI phase. Reaching the equilibrium during crystallization requires longer simulation times, especially when methane molecules form a bubble in water (Fig. 1). In our calculations, we consider only those cases when hydrate melts and equilibrium establishes much faster, during a few nanoseconds. When the volume of the sI phase stops changing we assume that the temperature and pressure in the system correspond to the coexistence conditions. Typical pressure and temperature evolution is shown in Fig. 2.

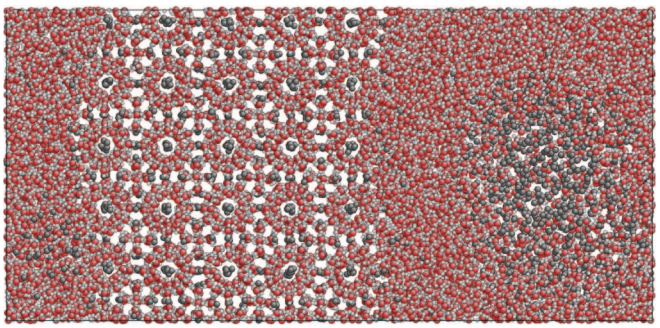

FIG. 1. A snapshot of the simulation box from the equilibrium MD trajectory during the phase coexistence simulation (red atoms – O, small grey atoms – H, dark grey atoms – CH_4). The microfaceted structure (Ref. 55) at the sI boundary are visible as well as the bubble of methane in water.

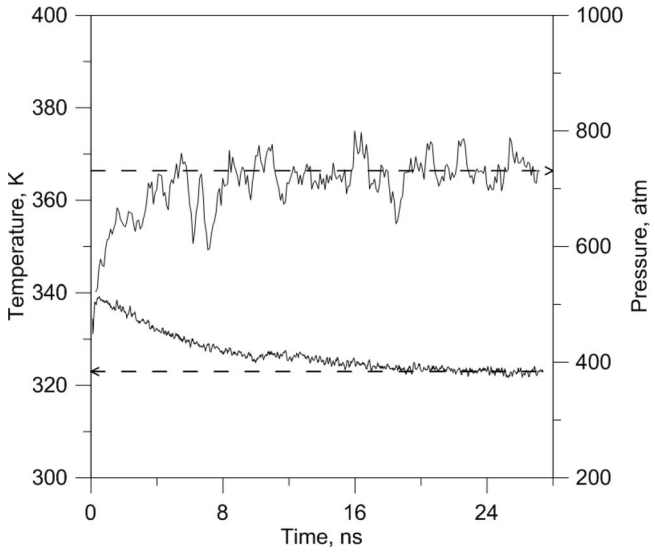

FIG. 2. Typical temperature (the lower curve) and pressure (the upper curve) evolution during phase coexistence simulations. Dashed lines show equilibrium temperature and pressure for the particular MD trajectory.

The typical simulation box in the previous studies of gas hydrates contains 2 × 2 × 2 or 2 × 2 × 4 unit cells. In our simulation, we use larger system sizes to decrease the possible influence of size effects. Our results for different water models (TIP4P/Ice, TIP4P/2005 and SPC/E) and different system sizes (5 × 5 × 10 unit cells — 36500 atoms, 3 × 3 × 6 unit cells — 7884 atoms) are shown in Fig. 3.

According to Conde and Vega,[37] the TIP4P/Ice model provides the best agreement with the experimental data. Jensen *et al.*[39] determined the sI melting line by free energy calculations via Monte Carlo method for TIP4P/Ice model and the agreement of their results is worse than it was found by Conde and Vega (although the LJ potentials for methane were slightly different). Our MD results are in agreement with the data of Jensen *et al.*[39] This is a strange fact because our results for TIP4P/2005 models are in a fairly good agreement with Conde and Vega.[37] We attribute this discrepancy to the larger interface area of our model (5 × 5 unit cells compared to 2 × 2 in Ref. 37). Presumably, smaller interface cross-sections can result in larger statistical uncertainty and biased coexisting pressure and temperature values. Our results show that the TIP4P/2005 model gives the better agreement with the experimental coexistence line than the TIP4P/Ice model in the entire pressure range considered. The coexistence temperature values are systematically 10–20 K lower for the former model but the qualitative curve shape reproduces the experimental data quite well.

IV. DECAY OF SUPERHEATED sI LATTICE

First order phase transitions allow the formation of metastable states. Metastability of gas hydrates is considered in the context of applications.[59,60] A concept of the spinodal is introduced to denote the stability limit of homogeneous phase. The thermodynamic criterion of the spinodal is $(\partial P/\partial\rho)_T = 0$. However, the thermodynamic spinodal can not be usually reached because of the kinetic instability caused by nucleation.

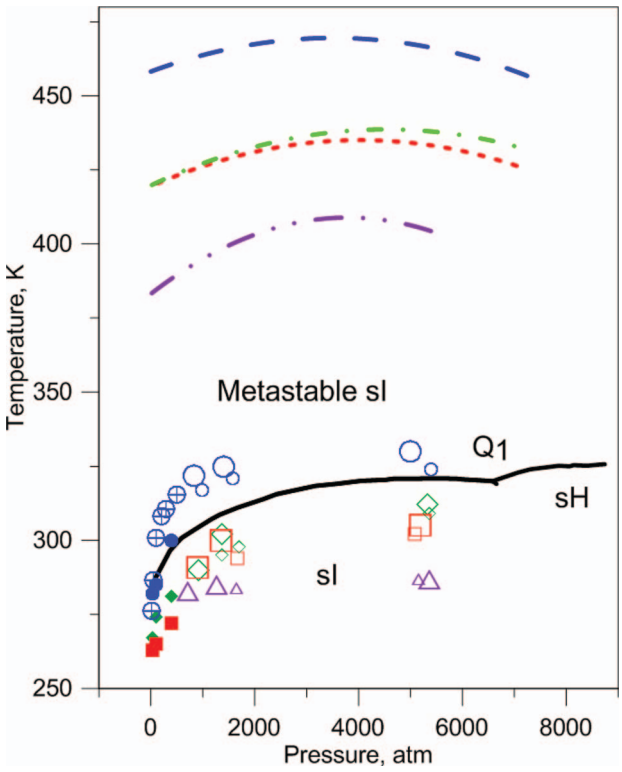

FIG. 3. Methane-water phase diagram. The solid line is the experimental (Ref. 56) three-phase equilibrium curve of methane hydrate. Q_1 is the quadruple point (sI methane hydrate – sH methane hydrate – liquid water – gaseous methane). The crossed circles show the result of Jensen *et al.* (Ref. 39) for TIP4P/Ice model. The filled blue, green, and red symbols show the three-phase coexistence points of Conde and Vega (Ref. 37) and open symbols show our results: purple triangles – SPC/E, green diamonds, and red squares – TIP4P/2005 with $\chi = 1.07$ and 1.00, respectively, blue circles – TIP4P/Ice. Big symbols correspond to $5 \times 5 \times 10$ unit cell systems and small symbols correspond to $3 \times 3 \times 6$ systems. Dashed lines show the kinetic stability boundaries at $\dot{T} = 1.5 \times 10^{12}$ K/s for different models (from bottom to top): SPC/E, TIP4P/2005 (no difference for $\chi = 1$ and 1.07) and TIP4P/Ice.

Melting is known to begin with heterogeneous nucleation at surfaces, grain boundaries and defects. However, the theoretical stability limit of a single crystal is determined by the homogeneous nucleation of liquid phase.[61–63] Rather unusual and special conditions are required to take solid to the corresponding highly metastable states experimentally. However, it seems to be possible in shock-wave experiments as it was argued for metals.[64]

Using the classical nucleation theory,[61] we can estimate an energy barrier for the homogeneous nucleation in sI methane hydrate as a work of a critical bubble formation $\Delta G^*(T) = 16\pi\gamma^3/[3(\Delta H_m(T_m - T)/T_m)^2]$, where γ is the interfacial energy, T_m is the equilibrium melting temperature and ΔH_m is the enthalpy of fusion per unit volume (for the estimates here we neglect the elastic energy considered in Ref. 61). The homogeneous nucleation rate as a function of temperature grows exponentially as $J \sim \exp(-\frac{\Delta G^*(T)}{kT})$. Small energy barrier values $\Delta G^*(T)/(kT) \lesssim 100$ manifest the kinetic stability limit.[65]

There are no data available on how methane dissolved in water influence the interfacial free energy. For the estimate, we use in this work the interfacial free energy between methane hydrate and water that is approximately[66] 3.9 $\times 10^{-2}$ J m^{-2}. During the homogeneous nucleation at the methane hydrate decay, the effective methane concentration is about $X_{CH_4} = 0.17$. An accurate estimate of the solid-liquid interface energy in this case is beyond the scope of this work. In Ref. 67, the authors present data on the hydrate formation nucleation rate for different aqueous mole fractions X_{CH_4} of methane. When methane concentration X_{CH_4} increases from 0.02 to 0.039, the nucleation rate J increases 5–10 times only. According to the classical nucleation theory, the nucleation barrier depends strongly on the interfacial energy $\Delta G^*(T) \sim \gamma^3$ that is why we can conclude that γ does not essentially depend on X_{CH_4}, at least for $0.02 < X_{CH_4} < 0.039$.

The enthalpy of fusion is 3.06 kJ/g.[1] At $P = 1$ bar the melting temperature is $T_m = 244$ K. At $T = T_m + 10$ K the ratio of the nucleation energy barrier to the average thermal energy is $\Delta G^*(T)/(kT) \sim 20$. This ratio corresponds to very high metastability of the solid phase that should be close to the spinodal decay. Thus, the classical nucleation theory predicts the maximum superheating of sI structure to be not more that 10 K.

The validity of the classical nucleation theory depends on how realistic its basic assumptions are. Namely, the spherical shape of the critical nucleus, the transient quasi-equilibrium between the nucleus and the ambient phase, the possibility to use macroscopic bulk properties for the ΔG^* estimate, etc. The direct MD simulation is free from such idealized assumptions and is able to give more realistic estimates of the stability boundary.

We consider an MD simulation box of $5 \times 5 \times 5$ unit cells of sI structure at different densities. The system is heated isochorically using gradual velocity rescaling. MD trajectories are computationally limited to the sub-microsecond scale that results in very high heating rates in the MD models. The corresponding isochores at $\dot{T} = 1.5 \times 10^{12}$ K/s can be seen in Fig. 4. While the atomic structure in the simulation box remains crystalline, the isochores change continuously with the gradual deviation from linearity. The decay of the crystalline methane hydrate into a water-methane mixture corresponds to a sudden break of an isochore. Three snapshots of the system illustrate this process (Fig. 4). The formation of a single nucleus can be distinguished in the $5 \times 5 \times 5$ system at visual inspection. However, periodic boundary conditions essentially influence the nucleus growth process.

The stability boundaries obtained in this way for different water models and 100 percent cage occupancy are shown in Fig. 3. The accuracy of the stability boundary estimates obtained in this work can be determined based of the accuracy of the coexistence curves obtained for the corresponding water models. The general conclusion we can make is that the superheating limit of the sI structure is much higher than it can be estimated from the classical nucleation theory and is about 2 times higher than was roughly predicted in Ref. 37.

It was shown in Ref. 62 that the superheated crystal decay temperature depends on the $\dot{T}/V$ ratio, where V is the volume of the simulation box. It means that one can reach smaller superheatings when the heating rate is lower or/and the volume of the system is larger because the probability of the new phase nucleation becomes higher. However, the very strong dependence of the homogeneous nucleation rate J on

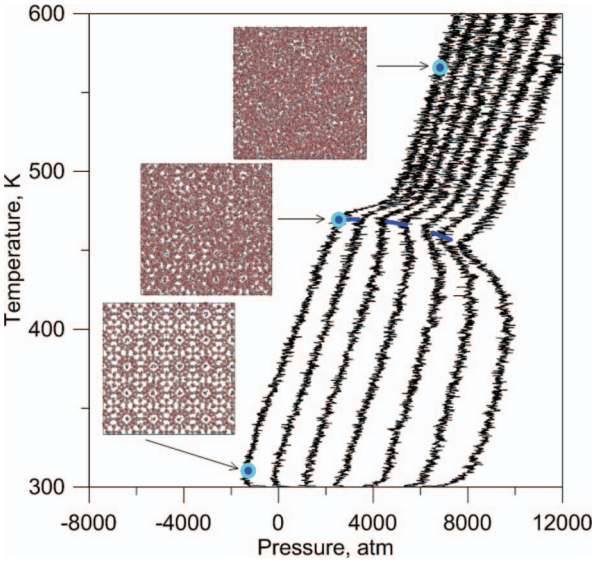

FIG. 4. Isochores and the kinetic stability boundary at $\dot{T} = 1.5 \times 10^{12}$ K/s (dashed line) for the TIP4P/Ice model. Density varies from 0.9056 to 0.9516 g/cc. Snapshots of the simulation box are shown for 3 representative states.

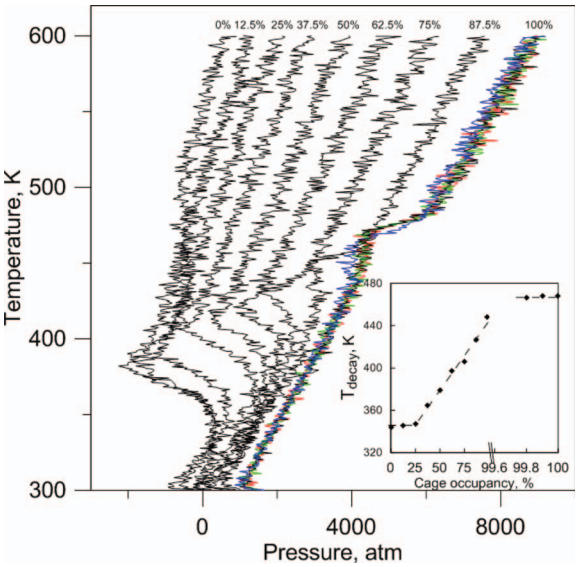

FIG. 6. The influence of the number of methane molecules on the decay temperature for the $5 \times 5 \times 5$ unit cell system and $\dot{T} = 1.5 \times 10^{12}$ K/s. Cage occupancy is shown in percents. The green isochore corresponds to the system without 1 CH_4, the red — without 2 CH_4, the blue — without 20 CH_4. The inset shows the decay temperature dependence on cage occupancy.

temperature contracts the interval of the decay temperature variation.

Our calculations for methane hydrate confirm these expectations. We fix the density of the system and vary the heating rate and the volume. If we increase the volume of the system ten times and decrease the heating rate ten times simultaneously, then the decay temperature should be the same. Corresponding isochores for different systems are shown in Fig. 5. The decrease of the $\dot{T}/V$ ratio from 6.9×10^7 K/s/Å^3 to 6.9×10^4 K/s/Å^3 corresponds to the decrease of the decay temperature from $\simeq$510 K to $\simeq$430 K (about 15 percent, see the inset in Fig. 5). Two isochores obtained for nearly the same $\dot{T}/V$ ratio and essentially different system sizes coincide (certainly fluctuations of pressure are smaller for the larger system). This fact indirectly confirms the applicability of homogeneous nucleation as a model of the sI structure decay in the single crystal case considered. The question of the extrapolation of T_{decay} at $\dot{T}/V \to 0$ is beyond the scope of this work and needs further study, as well as the question of multi-bubble homogeneous nucleation in larger systems (e.g., see Ref. 68).

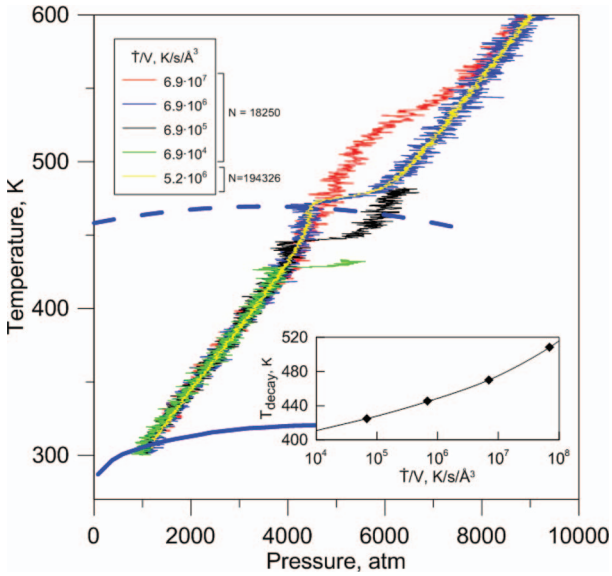

FIG. 5. Isochores for 0.9194 g/cc and different $\dot{T}/V$. The yellow isochore corresponds to the $11 \times 11 \times 11$ unit cells system, other isochores correspond to the $5 \times 5 \times 5$ system. The inset shows the decay temperature dependence on $\dot{T}/V$. The solid and dashed curves show the melting line and the kinetic stability boundary for TIP4P/Ice model as in Fig. 3.

Removing of a methane molecule from a water cage creates a defect in sI crystal lattice. To determine importance of this effect, we carry out calculations of isochores at different cage occupancy. We consider an MD simulation box of $5 \times 5 \times 5$ unit cells at 0.9194 g/cc. Such simulation box contains 1000 water cages with 1000 methane molecules at full occupancy. A fixed number of random methane molecules is deleted from the simulation box. There is no difference between the results when we delete one (green line in Fig. 6) or two (red line) molecules. Small changes are observed when 20 methane molecules are deleted from the simulation box (blue line). With a further decrease in the number of methane molecules the decay temperature decreases too (see the inset in Fig. 6). The decay temperature is constant for systems with low cage occupancy because the sI lattice becomes unstable.

V. CONCLUSIONS

We calculated the solid-liquid coexistence curve for sI methane hydrate using different water models in the 0-5000 bar pressure range. Our results correct the previously claimed[37] good performance of the TIP4P/Ice model at low pressures but agree with the results of Ref. 39. The kinetic stability boundary due to homogeneous nucleation was determined for the sI structure. Contrary to the predictions

of the classical nucleation theory the perfect sI lattice can endure large superheatings. The universal dependence of the kinetic stability boundary on the heating rate and the system volume was revealed. It was shown that the decrease of cage occupancy systematically lowers the decay temperature.

ACKNOWLEDGMENTS

This work was financially supported by the Russian Foundation for Basic Research Grants 09-08-01116 and 11-01-12131-ofi-m and the President of RF Grant MK-6719.2010.8 (V.V.S.) Simulations were carried out using the computing cluster "Lomonosov" of the Moscow State University and the MIPT-60 cluster of the Moscow Institute of Physics and Technology.

[1]E. D. Sloan and C. A. Koh, *Clathrate Hydrates of Natural Gases*, 3rd ed. (CRC, Boca Raton, FL, 2008), p. 752.
[2]E. G. Hammerschmidt, Ind. Eng. Chem. **26**, 851 (1934).
[3]N. Iro, D. Gautier, F. Hersant, D. Bockelée-Morvan, and J. I. Lunine, Icarus **161**, 511 (2003).
[4]S. W. Kieffer, X. Lu, C. M. Bethke, J. R. Spencer, S. Marshak, and A. Navrotsky, Science **314**, 1764 (2006).
[5]R. K. McMullan and G. A. Jeffrey, J. Chem. Phys. **42**, 2725 (1965).
[6]T. C.W. Mak and R. K. McMullan, J. Chem. Phys. **42**, 2732 (1965).
[7]J. Ripmeester, J. Tse, C. Ratcliffe, and B. Powell, Nature (London) **325**, 135 (1987).
[8]J. P. Kennett, K. G. Cannariato, I. L. Hendy, and R. J. Behl, *Methane Hydrates in Quaternary Climate Change: The Clathrate Gun Hypothesis* (American Geophysical Union, Washington, DC, 2003), p. 216.
[9]J. P. Long and E. D. Sloan, Int. J. Thermophys. **17**, 1 (1996).
[10]I. Aya, K. Yamane, and H. Nariai, Energy **22**, 263 (1997).
[11]R. P. Warzinski, R. J. Lynn, and G. D. Holder, Ann. N.Y. Acad. Sci. **912**, 226 (2000).
[12]H. Herzog, K. Caldeira, and E. Adams, in *Encyclopedia of Ocean Sciences*, edited by J. H. Steele (Academic, Oxford, 2001), pp. 408–414.
[13]E. M. Yezdimer, P. T. Cummings, and A. A. Chialvo, J. Phys. Chem. A **106**, 7982 (2002).
[14]L. J. Florusse, C. J. Peters, J. Schoonman, K. C. Hester, C. A. Koh, S. F. Dec, K. N. Marsh, and E. D. Sloan, Science **306**, 469 (2004).
[15]H. Lee, J. Lee, D. Y. Kim, J. Park, Y. Seo, H. Zeng, I. L. Moudrakovski, C. I. Ratcliffe, and J. A. Ripmeester, Nature (London) **434**, 743 (2005).
[16]F. Schuth, Nature (London) **434**, 712 (2005).
[17]T. A. Strobel, C. A. Koh, and E. D. Sloan, J. Phys. Chem. B **112**, 1885 (2008).
[18]A. Martin and C. J. Peters, J. Phys. Chem. B **113**, 7558 (2009).
[19]C. A. Koh, A. K. Sum, and E. D. Sloan, J. Appl. Phys. **106**, 061101 (2009).
[20]V. E. Antonov, V. S. Efimchenko, and M. Tkacz, J. Phys. Chem. B **113**, 779 (2009).
[21]P. M. Rodger, T. R. Forester, and W. Smith, Fluid Phase Equilib. **116**, 326 (1996).
[22]C. Moon, P. C. Taylor, and P. M. Rodger, J. Am. Chem. Soc. **125**, 4706 (2003).
[23]N. J. English and J. M. D. MacElroy, J. Chem. Phys. **120**, 10247 (2004).
[24]N. J. English, J. K. Johnson, and C. E. Taylor, J. Chem. Phys. **123**, 244503 (2005).
[25]H. Nada, J. Phys. Chem. B **110**, 16526 (2006).
[26]J. Vatamanu and P. G. Kusalik, J. Phys. Chem. B **110**, 15896 (2006).
[27]G. Guo, Y. Zhang, and H. Liu, J. Phys. Chem. C **111**, 2595 (2007).
[28]V. V. Sizov and E. M. Piotrovskaya, J. Phys. Chem. B **111**, 2886 (2007).
[29]O. Subbotin, V. Belosludov, E. Brodskaya, E. Piotrovskaya, and V. Sizov, Rus. J. Phys. Chem. A **82**, 1303 (2008).
[30]G. Guo, Y. Zhang, M. Li, and C. Wu, J. Chem. Phys. **128**, 194504 (2008).
[31]M. R. Walsh, C. A. Koh, E. D. Sloan, A. K. Sum, and D. T. Wu, Science **326**, 1095 (2009).
[32]N. J. English and G. M. Phelan, J. Chem. Phys. **131**, 074704 (2009).
[33]E. M. Myshakin, H. Jiang, R. P. Warzinski, and K. D. Jordan, J. Phys. Chem. A **113**, 1913 (2009).
[34]Y. Tung, L. Chen, Y. Chen, and S. Lin, J. Phys. Chem. B **114**, 10804 (2010).
[35]W. L. Jorgensen, J. Chandrasekhar, J. D. Madura, R. W. Impey, and M. L. Klein, J. Chem. Phys. **79**, 926 (1983).
[36]W. L. Jorgensen, D. S. Maxwell, and J. Tirado-Rives, J. Am. Chem. Soc. **118**, 11225 (1996).
[37]M. M. Conde and C. Vega, J. Chem. Phys. **133**, 064507 (2010).
[38]J. L. F. Abascal, E. Sanz, R. G. Fernández, and C. Vega, J. Chem. Phys. **122**, 234511 (2005).
[39]L. Jensen, K. Thomsen, N. von Solms, S. Wierzchowski, M. R. Walsh, C. A. Koh, E. D. Sloan, D. T. Wu, and A. K. Sum, J. Phys. Chem. B **114**, 5775 (2010).
[40]C. Gutt, B. Asmussen, W. Press, M. R. Johnson, Y. P. Handa, and J. S. Tse, J. Chem. Phys. **113**, 4713 (2000).
[41]J. A. Hayward and J. R. Reimers, J. Chem. Phys. **106**, 1518 (1997).
[42]C. Vega, E. Sanz, J. L. F. Abascal, and E. G. Noya, J. Phys.: Condens. Matter. **20**, 153101 (2008).
[43]N. Gribova, Y. Fomin, D. Frenkel, and V. Ryzhov, Phys. Rev. E **79**, 1 (2009).
[44]Y. Fomin and V. Ryzhov, Phys. Lett. A **375**, 2181 (2011).
[45]Y. D. Fomin, E. N. Tsiok, and V. N. Ryzhov, J. Chem. Phys. **135**, 124512 (2011).
[46]H. Jiang, K. D. Jordan, and C. E. Taylor, J. Phys. Chem. B **111**, 6486 (2007).
[47]J. L. F. Abascal and C. Vega, J. Chem. Phys. **123**, 234505 (2005).
[48]H. J. C. Berendsen, J. R. Grigera, and T. P. Straatsma, J. Phys. Chem. **91**, 6269 (1987).
[49]B. Guillot and Y. Guissani, J. Chem. Phys. **99**, 8075 (1993).
[50]D. Paschek, J. Chem. Phys. **120**, 6674 (2004).
[51]R. Sun and Z. Duan, Geochim. Cosmochim. Acta **69**, 4411 (2005).
[52]H. Docherty, A. Galindo, C. Vega, and E. Sanz, J. Chem. Phys. **125**, 074510 (2006).
[53]R. W. Hockney and J. W. Eastwood, *Computer Simulation Using Particles* (McGraw-Hill, New York, 1981).
[54]S. Plimpton, J. Comput. Phys. **117**, 1 (1995).
[55]S. Liang and P. G. Kusalik, J. Phys. Chem. B **114**, 9563 (2010).
[56]Y. A. Dyadin, E. Y. Aladko, and E. G. Larionov, Mendeleev Communications **7**, 34 (1997).
[57]J. R. Morris, C. Z. Wang, K. M. Ho, and C. T. Chan, Phys. Rev. B **49**, 3109 (1994).
[58]S. V. Starikov and V. V. Stegailov, Phys. Rev. B **80**, 220104 (2009).
[59]V. Istomin, V. Kvon, and V. Durov, Gas Ind. Russ. **4**, 13 (2006), available online at http://www.gas-journal.ru/dgir/dgir_detailed_work.php?DGIR_ELEMENT_ID=283&WORK_ELEMENT_ID=5643.
[60]V. Istomin, V. Yakushev, N. Makhonina, V. Kwon, and E. Chuvilin, Gas Ind. Russ. **4**, 16 (2006), available online at http://www.gas-journal.ru/dgir/dgir_detailed_work.php?DGIR_ELEMENT_ID=283&WORK_ELEMENT_ID=5645.
[61]K. Lu and Y. Li, Phys. Rev. Lett. **80**, 4474 (1998).
[62]G. E. Norman and V. V. Stegailov, Mol. Simul. **30**, 397 (2004).
[63]A. Kuksin, G. Norman, and V. Stegailov, High Temp. **45**, 37 (2007).
[64]S. Luo and T. J. Ahrens, Appl. Phys. Lett. **82**, 1836 (2003).
[65]J. Schmelzer, *Nucleation Theory and Applications* (Wiley-VCH, Berlin, 2005).
[66]T. Uchida, T. Ebinuma, and T. Ishizaki, J. Phys. Chem. B **103**, 3659 (1999).
[67]M. R. Walsh, G. T. Beckham, C. A. Koh, E. D. Sloan, D. T. Wu, and A. K. Sum, J. Phys. Chem. C **115**, 21241 (2011).
[68]A. Kuksin, G. Norman, V. Pisarev, V. Stegailov, and A. Yanilkin, Phys. Rev. B **82**, 174101 (2010).